ISSN: 2578-7365

Research Article

Journal of Chemistry: Education, Research and Practice

Development and Characterization of Silicon Carbide Coating on Graphite Substrate

F Z Mohammad*, M Akhtar Sharif, M Anas Ahmed, Muhammad Suhail

Center of Excellence in Science and Applied Technologies, Islamabad, Pakistan

***Corresponding author**
F Z Mohammad, Centre of Excellence in Science and Applied Technologies, Islamabad, Pakistan.

Submitted: 19 May 2022; **Accepted:** 27 May 2022; **Published:** 15 Jul 2022

Citation: *F Z Mohammad, M Akhtar Sharif, M Anas Ahmed, Muhammad Suhail. (2022). Development and Characterization of Silicon Carbide Coating on Graphite Substrate. J Chem Edu Res Prac, 6(2), 258-266.*

Abstract

The development of materials with unique and improved properties using low cost processes is essential to increase performance and reduce cost of the solid rocket motors. Specifically, advancements are needed for boost phase nozzle. As these motors operate at very high pressure and temperatures, the nozzle must survive high thermal stresses with minimal erosion to maintain performance. Currently three material choices are being exploited; which are refractory metals, graphite and carbon-carbon composites. Of these three materials graphite is the most attractive choice because of its low cost, light weight, and easy forming. However, graphite is prone to erosion, both chemical and mechanical, which may affect the ballistic conditions and mechanical properties of the nozzle. To minimize this erosion Pyrolytic Graphite (PG) coating inside the nozzle is used. However, PG coating is prone to cracking and spallation along with very cumbersome deposition process. Another possible methodology to avoid this erosion is to convert the inside surface of the rocket nozzle to Silicon Carbide (SiC), which is very erosion resistant and have much better thermal stability compared to graphite and even PG. Due to its functionally gradient nature such a layer will be very adherent and resistant to spallation. Despite its very good adhesion due to its functionally gradient nature, this layer due to its porous nature exhibit poor oxidation performance compared to a dense SiC layer. The current research is focused on synthesizing, characterizing and oxidation testing of a bi-layer; a functionally gradient inner layer and dense outer layer, SiC coating on graphite.

Keywords: SiC Coating, Graphite, Oxidation, Rocket Nozzle, Pack Cementation

Introduction

Rocket motor nozzles are subjected to severe environmental and oxidative conditions. Temperature there is in the range of 3000 ˚K and pressure is somewhat near 5 MPa [1]. To withstand such demanding conditions there are only two materials choices namely-Refractory metals and carbon/graphite materials. But due to its high specific strength (low density) and higher melting point carbon materials are preferred [2, 3]. But carbon materials have tendency to oxidize at temperatures above 500 ˚C [4-7]. This oxidation results in loss of mechanical properties such as UTS, YS, Kic and stored strain energy [8].

Theoretical density of graphite is 2.26 g/cm^3, while the densities of most of the synthetic commercial graphite materials fall in the range of 1.6- 1.9 g/cm^3, which means they contain about 15-30 % porosity [9]. The major part of this porosity usually consists of open interconnected pores allowing an oxidizing environment to exist throughout the material [10].

In graphite, oxidation takes place only on active carbon sites and the rate of oxidation depends upon the density and accessibility of these active sites [11]. In graphite, these oxidation active sites exist on the edges of basal planes.

Oxidation of graphite above a certain threshold temperature (which depends upon the grade of graphite, and it ranges between 800-1000 K) results in mass loss and microstructural deterioration (crack development, enlargement of pores, and de-bonding between material components). Both mass loss and microstructure deterioration reduces the mechanical strength and toughness of the material [12, 13].

In rocket nozzle case different oxidants are produced as a result of the combustion of propellant. The most important oxidants involved in the chemical recession of nozzle material are H_2, H_2O, CO_2, CO and OH [1]. Recession is most pronounced in the throat region which may change the ballistic performance. Recession rate (mm/sec) can be approximated by [1]:

$$R = 0.0318\ N_{H2O} P^{0.8} \quad (1)$$

N_{H20} = Mole Fraction of H_20 present, P = Chamber Pressure in MPa

Mechanical erosion of graphite is only a fraction of the total erosion; rather mechanical erosion follows the chemical erosion.

Main exhaust specie which can cause mechanical erosion is Al2O3 particles, which have been reported, in some cases, stick to the graphite surface and this inhibit further gasification.

Oxidation alters the micro-mechanism involved in fracture behaviour of graphite. After oxidation both parameters Kic and γic (critical stain energy) are reduced. Critical strain energy reflects the total energy required to create 1 m2 of primary crack surface. Generally, there is a decrease in γic of about 30, 50, and 65 % for burn off of about 5, 10, and 20 % [8].

Some oxidation protection mechanism will really be greatly useful to retain its mechanical properties at high temperature and to avoid any erosion. SiC coating having good antioxidation properties is one of the most potential options to avoid or delay graphite oxidation inside the nozzle. Silicon carbide is covalently bonded carbide, having all the characteristics of a refractory material, in which a carbon atom is bonded with a silicon atom by sharing pairs of electrons and like all covalent bonds has a definite bond angle [14].

The oxidation behaviour of SiC can be divided into two categories: Passive and Active. Passive oxidation forms a coherent dense SiO_2 layer on the surface which drastically reduces the oxidation rate.

On the contrary active oxidation forms gaseous SiO, which dissipates away and oxidation becomes severe. The temperature at which oxidation changes from passive to active mode decrease with decrease in the oxygen partial pressure.

SiC deposited directly on to the graphite surface is prone to spallation due to CTE mismatch & poor adhesion [14]. To overcome this problem a surface layer of graphite is converted to SiC. There are many possible ways to make this converted SiC layer, but pack cementation is an easy and robust way to produce such a layer.

In the pack cementation process, the substrate to be coated is buried into a powder, upon heating a gaseous precursor is generated from within the powder and reaches the surface of the substrate and form a thin coating there [15].

The pack cementation technique to deposit SiC is very promising method, because it produces a naturally gradient layer of SiC on graphite surface having decreased coefficient of thermal expansion mismatch, it is simple and easy to monitor [16-18]. In the cementation process the gaseous reactive species are generated very close to the part to be coated from a condensed compound, usually called the cement. [19].

In pack cementation coating of SiC both Si and C can be generated by the cement.

Alternatively SiC deposition on the graphite substrate can also be obtained via a reaction in which the carbon is provided by the substrate itself. Thus, the only gaseous precursor needed is Si containing species [19].

Depending upon the temperature and partial pressure of O_2 there may be two types of reactions [20]. Passive oxidation occurring for a higher O_2 partial pressure and low temperatures which results in the formation of SiO_2

$$SiC + 3/2\ O_2 \longrightarrow SiO_2 + CO \qquad (a)$$

For lower partial pressures of O_2 and/or high temperature an active oxidation takes place which results in the strong ablation of SiC, according to the following reaction.

$$SiC + O_2 \longrightarrow SiO\ (g) + CO \qquad (b)$$

During the SiC deposition the following chain of reactions takes place [21]:

- Vaporization and decomposition of SiO_2
- Diffusion of the formed SiO through pores.

When the cementation reaction starts, the gaseous Si precursor SiO (g) may react directly with the free surface of the carbon substrate to form SiC. As soon as the surface is fully covered with SiC, a diffusion phenomenon must occur to further permit the film growth. Depending upon the diffusivity of the diffusing species two possible situation may be observed. The reaction may take place at:

- C-SiC interface
- At the outer SiC surface

In both cases, the coating thickness is related to the diffusion distance of the rate limiting specie and thus a decrease in growth rate should be observed as a function of cementation duration and co-workers have established that the reaction takes place at C-SiC interface, thus it is an inward grown coating [22]. SiC coating obtained through pack cementation process is porous in nature due to the formation of CO as a by-product during the reactions.

This porous surface alone does not ideally protect the graphite from oxidation and can result in catastrophic failure in order to avoid this ideally multilayer coating is develop [12]. Thus, a second denser layer of SiC is applied over the first one through slurry method. This method involves dipping of samples in homogenous slurry, composed of phenolic resin and Si powder, followed by heating at high temperature to form dense, uniform and pore free coating. Such bi-layer; a functionally gradient inner layer and dense outer layer, SiC coating on graphite provides good oxidation and erosion resistance.

Experimental Work

The feasibility of a chemical reaction can be determined by calculating the Gibbs free energy ΔGr of the reaction at a given temperature and pressure. In order to calculate Gibb's free energy of the reaction first we need to calculate the free energy of formation, ΔG_f, for the individual species of the reactants and products. This can be done by the equation:

$$\Delta G_f(T) = \Delta H^\circ_f(298) + \int_{298}^{T} C_p\, dT - TS^\circ(298) - \int_{298}^{T} (Cp/T)dT$$

The free energy of the reaction is calculated as

$$\Delta G_r = \Delta G_f \text{ (Product)} - \Delta G_f \text{ (Reactant)}$$

A reaction will occur only when ΔGr value is negative; when positive the reaction will not take place, or may progress in the reverse direction.

A CVD phase diagram can be constructed at constant temperature or pressure either using the equilibrium constant or the minimization of Gibbs free energy method. The equilibrium constant method requires the information on all reactive species and the chemical reactions involves the use of non-linear equations. The minimization of Gibbs free energy method involves the use of linear equations and it is independent of reaction path [15].

Based on these principles different computer programs are available to calculate and construct a CVD phase diagram. During the current study MTDATA was used to construct the CVD phase diagram. Two constructed phase diagrams at two different pressures are shown in Fig 1 and Fig 2

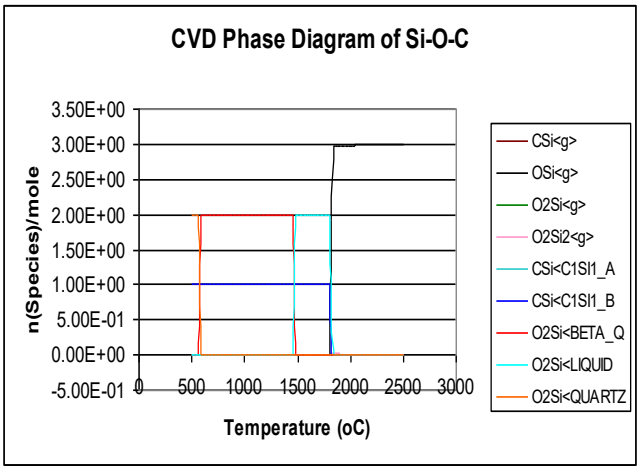

Figure 1: CVD phase Diagram at Atmospheric Pressure

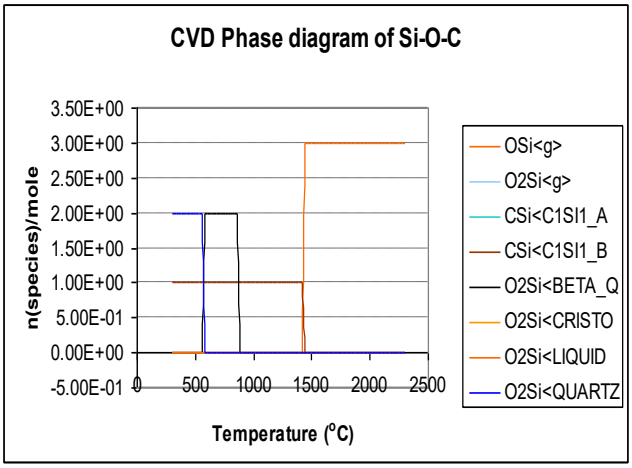

Figure 2: CVD Phase Diagram at Sub-Atmospheric Pressure (104 KPa)

These phase diagrams show that the precursor phase, SiO, begins to generate from within the cement at about 1800 °C under atmospheric pressure conditions, and at about 1450 °C under low pressure (104 kPa) conditions. Whether it is overall process pressure or the partial pressure of oxygen that has lowered the SiO generation temperature. Paccaud and co-workers concluded that during the pack cementation of SiC coatings following reactions takes place in sequence [21]. The same reaction has also been quoted in reference [23].

$$SiO_2 \longrightarrow SiO + \tfrac{1}{2} O_2 \quad \text{(c)}$$

This molecular oxygen then diffuses through the cement to react with SiC [23]. The oxidation of SiC can be either active or passive, depending upon the partial pressure of O2 and the process temperature.

$$SiC + 3/2\ O_2 \longrightarrow SiO_2 + CO \quad \text{(Passive oxidation)} \quad \text{(d)}$$

$$SiC + O_2 \longrightarrow SiO + CO \quad \text{(Active oxidation)} \quad \text{(e)}$$

This explanation suggests that it is the partial pressure of oxygen rather than the process pressure that has lowered the SiO generation temperature. The oxygen partial pressure can be lowered by depositing the coating under an inert gas atmosphere.

Although CVD phase diagrams can provide vital information as to the equilibrium phases and the amount of solid and gaseous species present in the system at a given temperature and pressure, the CVD processes are non-equilibrium in nature therefore these diagrams can be used only to provide a guideline for selecting the process conditions, whether a coating forms or not will depend on the kinetics of the reaction.

Pack Cementation Process

To deposit first; gradient layer graphite samples were buried in a cement comprised of 95% Al2O3 and 5% SiO2. Cement was prepared by using powders of Al2O3 and SiO2 of the size 300 mesh in a TURBULA mixture. To ensure the homogeneity of the cement it was mixed in TURBULA mixture for 12 hrs.

To make sure that sample get a homogenous thickness of coating, a 5 mm thick layer of cement was placed all around the sample in an alumina crucible. Then it was heated to 1550˚C for three hours under inert environment. To obtain the maximum thickness of converted SiC coating, processing time of three hours was selected.

After a specific dwelling time at the processing temperature, the crucible was allowed to cool down in the furnace. Finally, the crucible was removed from the furnace and the samples were again thoroughly cleaned and characterized again.

Slurry Method

Second layer was developed over pack cementation coated substrates. Composition of 60 wt. % phenolic resin powder, 40 wt. % Si powder were mixed mechanically in ethanol. Pack cementation coated samples were dipped in slurry and oven dried at 60˚C for 3h to obtain green slurry coated samples. These samples were then heated in an inert atmosphere furnace according to the thermal cycle given in Fig 3. Under the Ar environment,

Si powder react with carbon yielded as a result of pyrolysis of phenolic resin to give smooth, uniform and pore free β-SiC layer. according to the below mentioned reaction.

$$Si\ (powder) + C\ (Phenolic\ resin) \longrightarrow SiC + Volatiles \quad (f)$$

The reaction starts at 1320 0C and ends at 1420 0C [24].

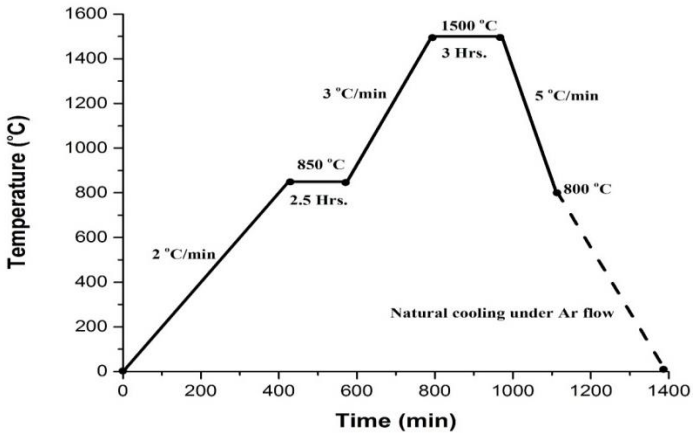

Figure 3: Thermal Cycle for Dense, Pore Free Coating

Results and Discussion

Crystalline Structure of Coating

While Crystalline structure of the coatings formed through pack cementation process and slurry method were studied using Bruker D8 Discovery X-ray diffractometers (XRD). From the XRD pattern Fig 4, it is confirmed that first coating formed on substrate possess carbon, silicon and β-SiC [25]. While the second coating composed of carbon, β-SiC and α-SiC [26] (Fig 5). XRD pattern also confirms the dense second coating because graphite peak diminishes.

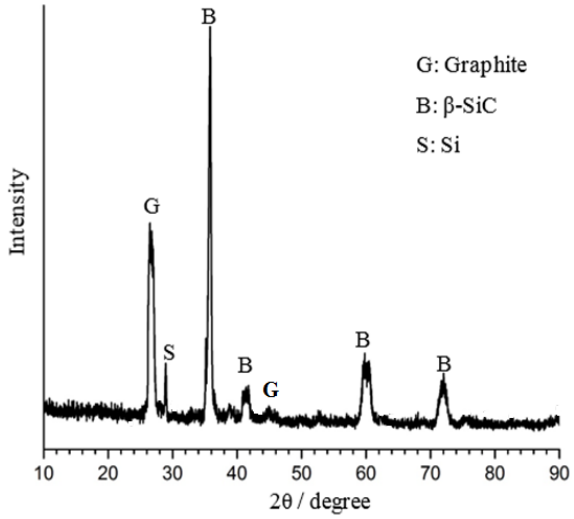

Figure 4: XRD Pattern of Converted SiC Coating

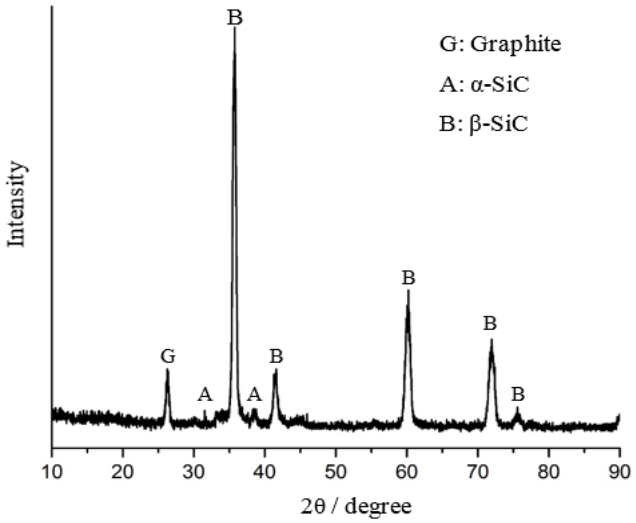

Figure 5: XRD Pattern of Second Coating

Microstructure of 1st and 2nd Coating

The converted SiC layer on graphite is an inward grown coating and its growth morphology depends upon the porosity in the substrate. As gaseous precursor, SiO diffuses through the pores and react with the graphite to form SiC according to the below mentioned reaction [18].

$$SiO + 2C \longrightarrow SiC + CO \quad (g)$$

As it moved down from the surface %age of graphite; that is converted to SiC. This gradient nature is very useful in avoiding possible spallation or cracking in the coating due to coefficient of thermal expansion (CTE) mismatch between the coating and the graphite substrate.

The silicon carbide formation is accompanied with the evolution of carbon monoxide [18]. The evolution of CO from the SiC-C interface results in the porosity of the converted SiC coating as shown in Fig 6. This porosity is very useful in redistributing stress generated due to CTE mismatch and thus prevents any cracking in the coating.

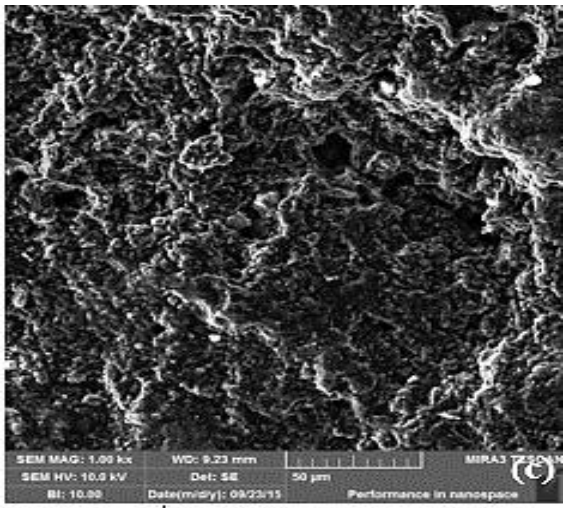

Figure 6: Top View of Converted SiC Layer on Graphite Substrate

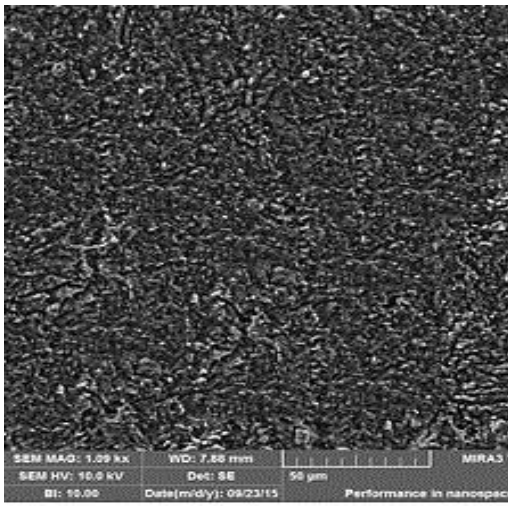

Figure 7: Top View of Second Coating

The surface topography of the second layer is shown in Fig-7 which shows that it is a dense, uniform and almost pore free coating. The thickness (approximately 90 µm) of the first layer is greater than the thickness (approximately 20 µm) of the second (denser) layer as shown in Fig-8. This bilayer coating is expected to provide better oxidation protection and resistance against spallation.

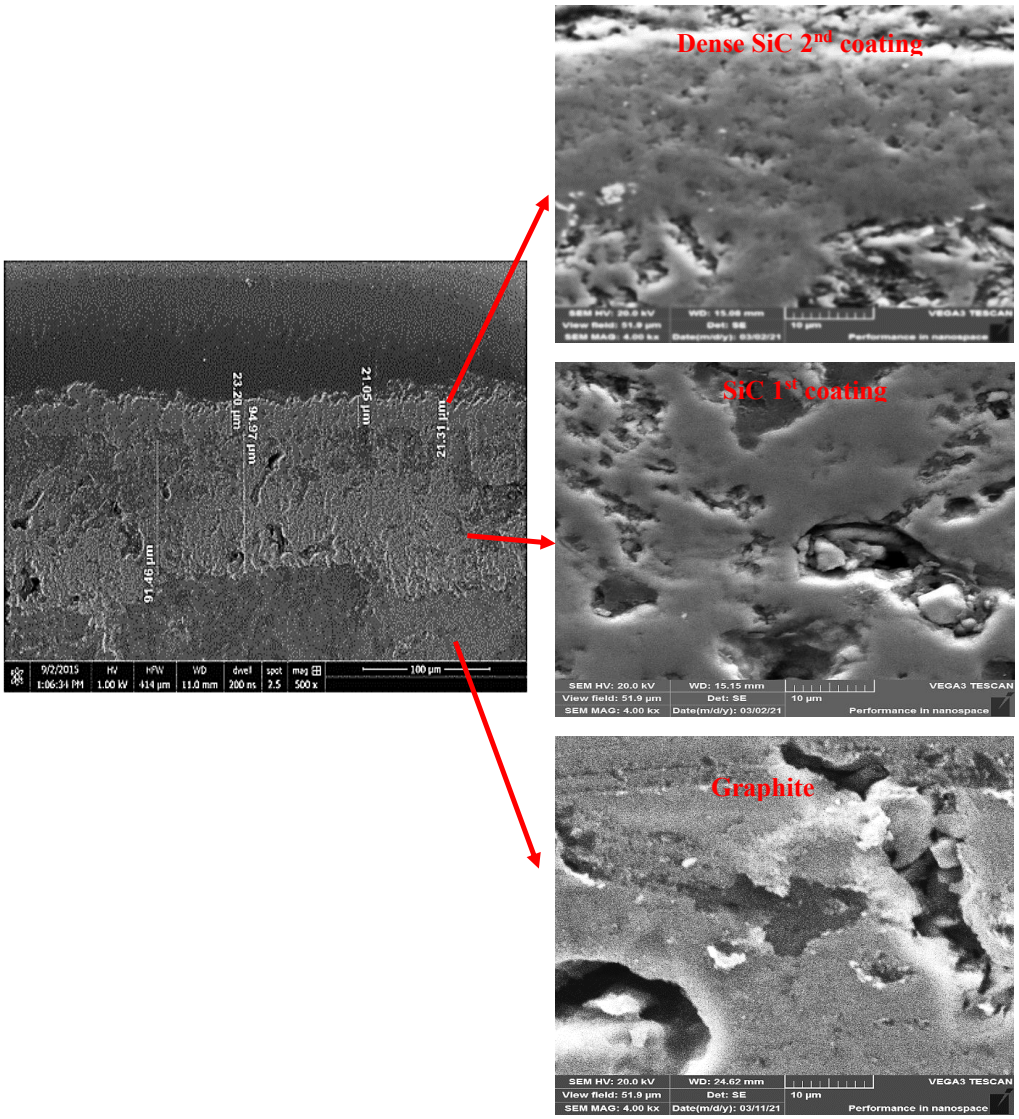

Figure 8: Cross Sectional Measurement of Bilayer Coating Thickness

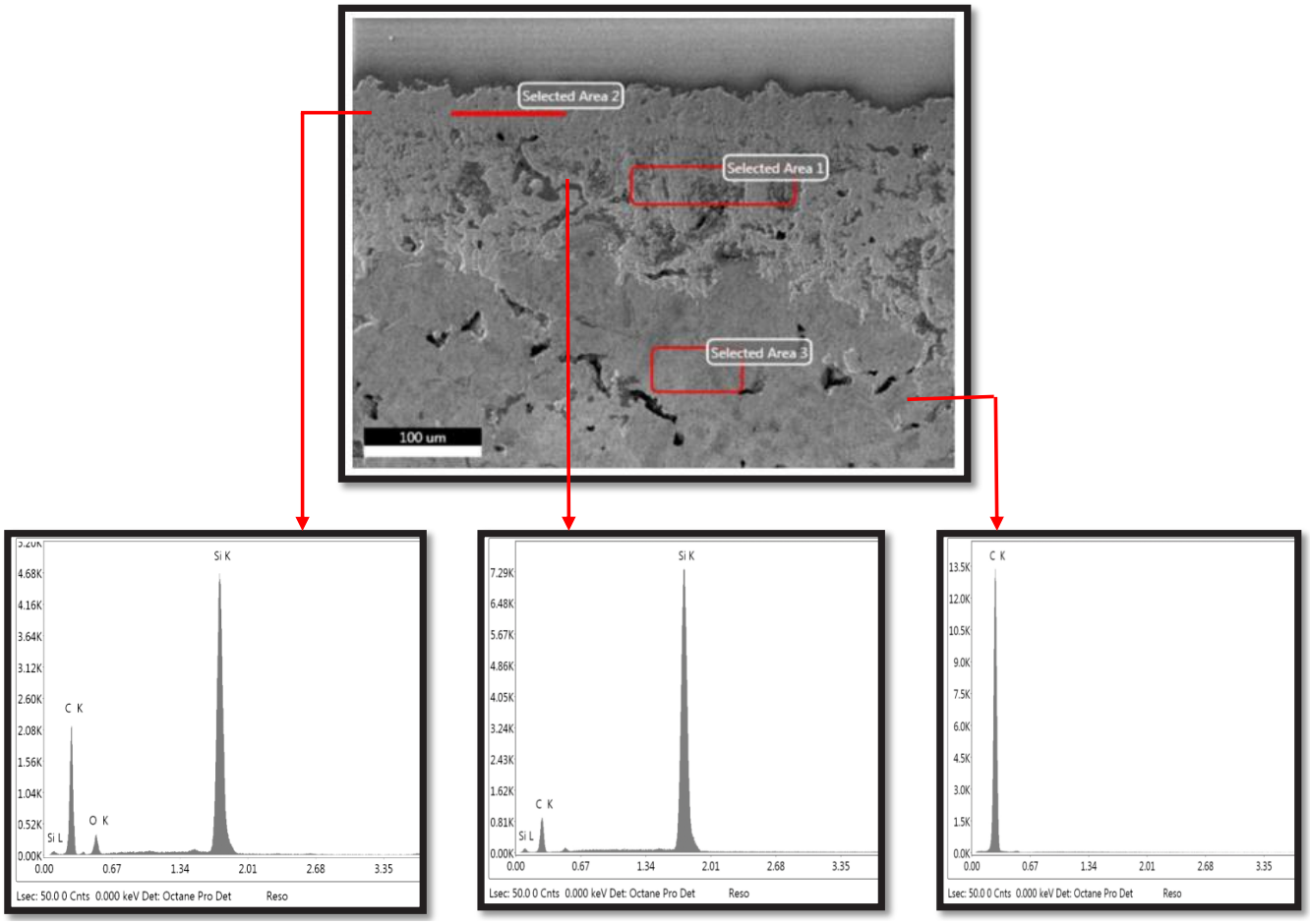

Figure 9: EDS Spectrum of Graphite, First Coating and Second Coating

EDS spectrum (Fig 9) obtained from analysis of the three different layers (substrate, first coating and second coating) shows differences in composition of these layers, pointing to functionally gradient coating.

A relation between processing time and thickness of the converted SiC coating is shown in Figure 10. The thickness of the coating increases linearly with increase in the processing time up to 135 minutes and then its growth rate begins to drop up to 180 minutes. The maximum coating thickness of 93µm was achieved at 180 minutes. After that there is a slight decrease in coating thickness for increasing the processing time. A slight decrease in coating thickness after a certain length of time may be explained that at higher temperatures SiC is very sensitive to oxidation, even at low partial pressure of oxygen; thus, any small amount of oxygen present in the system can cause active oxidation of SiC.

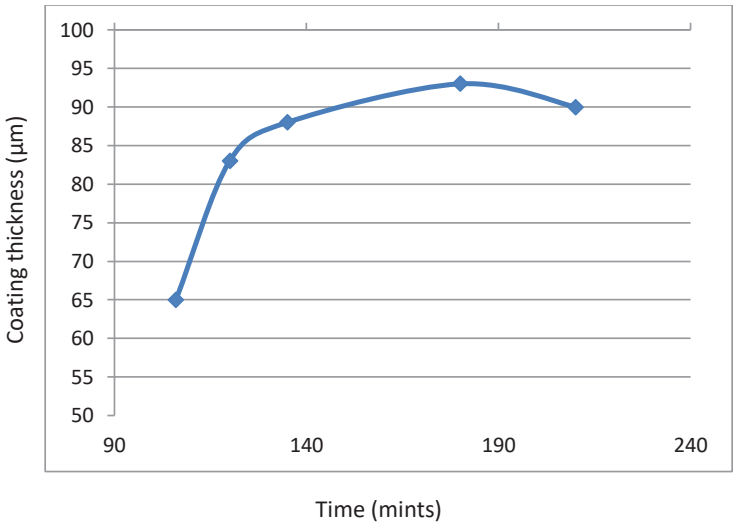

Figure 10: Relation Between Processing Time and The Coating Thickness

The continuous decrease in the growth rate of SiC layer with increase in processing time may be due to two reasons:
1. SiO_2 depleted volume has formed around the cemented part, which cause a decrease in partial pressure of SiO at the coating surface, due to increased diffusion distance;
2. Increase in coating thickness provides a longer diffusion path for SiO to reach the SiC-C interface, thus decrease the growth rate [27, 28].

Paccaud and co-workers found that the effect of coating thickness on the coating growth rate becomes noticeable only when the thickness of the coating is between 50-100 μm [21]. Below that thickness value, it is SiO2 depletion around the cemented sample that is responsible for the decrease in coating growth rate. The thickness of the converted SiC coating also depends upon the density of the substrate.

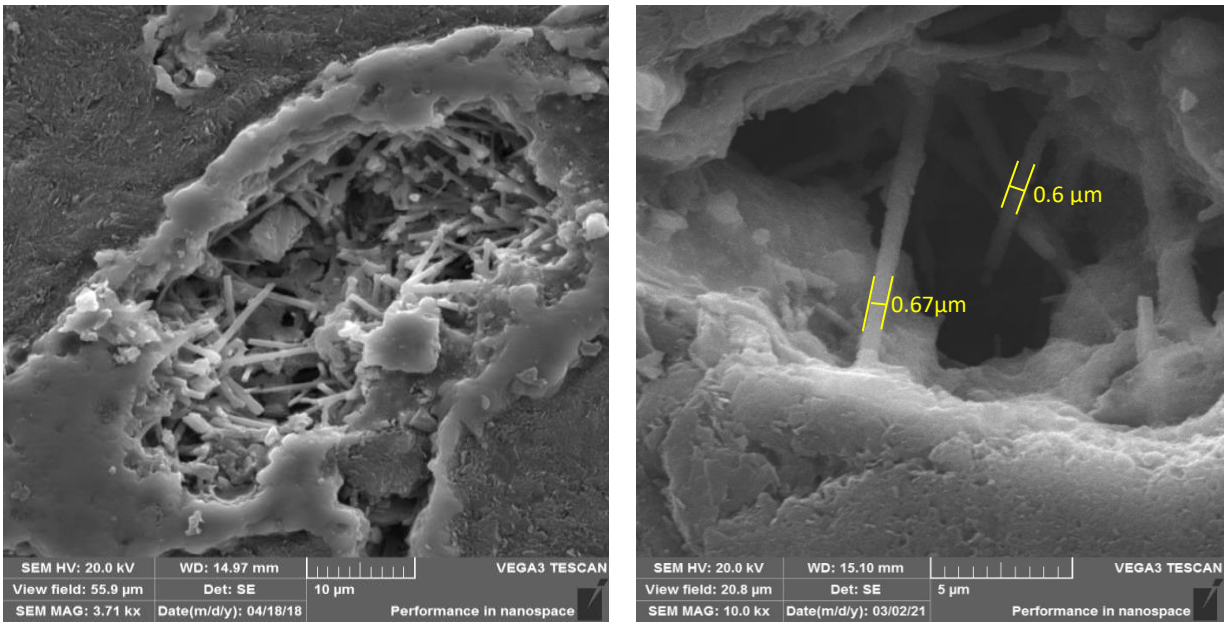

Figure 11: Sic Whiskers in Pores of Graphite Having Average Size of ~ 0.63 Microns

Another observation made during this research is the formation of SiC whiskers in substrate pores as shown in Fig 11. These whiskers are formed as a result of reaction between SiO and CO. Generally, the growth mechanisms of SiC whiskers involved vapour–solid (VS) reaction. VS mechanism involves Si containing vapours such as SiO (g) react with CO (g) or C(s) to form SiC nucleus and the whiskers or nano wires grow along the directions of the least stable plane [29, 30].

The growth of whiskers takes place according to the following reactions.

$$SiO\ (g) + 2C\ (s) \longrightarrow SiC\ (nucleus) + CO \quad (h)$$

$$SiO\ (g) + 3CO\ (g) \longrightarrow SiC\ (Whiskers) + 2CO_2 \quad (i)$$

Oxidation Testing

Oxidation testing of these samples were performed at (a) 500 °C, (b) 800 °C and (c) 1100 °C, respectively. The weight loss of uncoated graphite, single layered coated graphite and doubled layer coated graphite samples at 1100 °C after 1 h of oxidation was 23.1, 10.8 and 3.76 wt % respectively, as shown in Fig 12. The better oxidation performance of double-layered coated samples clearly indicates the effectiveness of top dense layer of SiC.

Generally, the mechanism of oxidation protection of the SiC layer on the carbon-based materials is given according to the reactions [18]:

$$2SiC + 3O2 \longrightarrow 2SiO2 + 2CO \quad (k)$$

$$SiC + 2O2 \longrightarrow SiO2 + CO2 \quad (l)$$

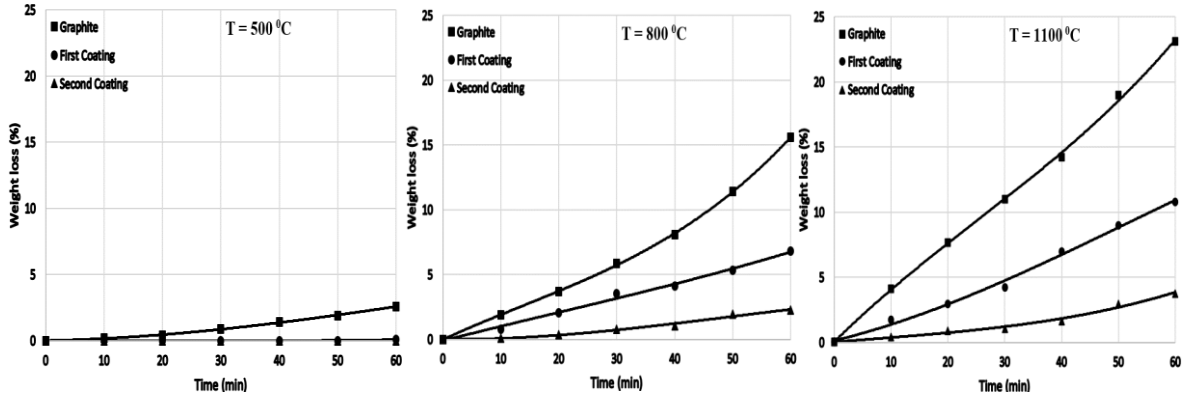

Figure 12: Oxidation Curve at 500 °C, 800 °C and 1100 °C

The oxidation performance of the double layer coated sample is even better than indicated by the weight loss data because we assume that this weight loss is mainly because of the cracks in the coating near the corner of the sample as shown in Fig 13. If corner of the sample is rounded there would be much better oxidation performance.

Figure 13: Corner Blistering After Cementation

Conclusions

During this research processing conditions were established to deposit a converted SiC layer on graphite surface. The characterization of synthesized layer showed that the layer was crystalline in nature and had a lot of micro porosity; which was inherent to the growth mechanism of this layer. A dense uniform and pore free coating formed over first coating by slurry method. Dual coating has better oxidation resistance than single coating done by pack cementation process. Overall coating thickness of about 115 µm was achieved with a first coating having a maximum penetration depth of 225 µm, which showed significant improvement in the oxidation resistant property of coating. Weight loss was decreased to 3.76 wt % from 23.1 wt % at 1100 ˚C for oxidation time of 1h. The weight loss of the coated samples has occurred because of mismatch in CTE of graphite and SiC coating that resulted in the cracking of SiC coating from sharp corners at elevated temperatures.

References

1. Jones, L. E., Thrower, P. A., & Walker Jr, P. L. (1986). Bulk graphite nozzle recession—an analysis based on the carbon-steam reaction. Carbon, 24(1), 43-49.
2. Abdollahi, A., Ehsani, N., Valefi, Z., & Khalifesoltani, A. (2017). SiC nanoparticles toughened-SiC/MoSi2-SiC multilayer functionally graded oxidation protective coating for carbon materials at high temperatures. Journal of Materials Engineering and Performance, 26(6), 2878-2889.
3. Wang, P., Han, W., Zhang, X., Li, N., Zhao, G., & Zhou, S. (2015). (ZrB2–SiC)/SiC oxidation protective coatings for graphite materials. Ceramics International, 41(5), 6941-6949.
4. Paul, B., Prakash, J., & Sarkar, P. S. (2015). Formation and characterization of uniform SiC coating on 3-D graphite substrate using halide activated pack cementation method. Surface and Coatings Technology, 282, 61-67.
5. Hatta, H., Goto, K., Sato, T., & Tanatsugu, N. (2003). Applications of carbon-carbon composites to an engine for a future space vehicle. Advanced Composite Materials, 12(2-3), 237-259.
6. Kobayashi, S., Wakayama, S., Aoki, T., & Hatta, H. (2003). Oxidation behavior and strength degradation of CVD-SiC coated C/C composites at high temperature in air. Advanced Composite Materials, 12(2-3), 171-183.
7. Sheehan, J. E. (1993). High-temperature coatings on carbon fibers and carbon-carbon composites. In Carbon–carbon materials and composites (pp. 223-266). William Andrew Publishing.
8. Wood, J. L., Bradt, R. C., & Walker Jr, P. L. (1980). Oxidation effects on toughness and slow crack growth in polycrystalline graphites. Carbon, 18(3), 179-189.
9. Sengupta, R., Bhattacharya, M., Bandyopadhyay, S., & Bhowmick, A. K. (2011). A review on the mechanical and electrical properties of graphite and modified graphite reinforced polymer composites. Progress in polymer science, 36(5), 638-670.
10. Thrower, P. A., Bognet, J. C., & Mathew, G. K. (1982). The influence of oxidation on the structure and strength of graphite-I: Materials of different structure. Carbon, 20(6), 457-464.
11. Hoffman, W. P., Phan, H. T., & Groszek, A. (1995). The deposition of silica on carbon as a model system for oxidation protection coatings. Carbon, 33(4), 509-524.
12. Semchenko, G., Shuteeva, I., Slepchenko, O., & Angolenko, L. (2005). Protection of graphite and graphite-containing materials from oxidation. Refractories & Industrial Ceramics, 46(4), 260–267.
13. Peng, T. C. (1979). Oxidation effects on the tensile strength

of ATJS graphite and vitreous carbon. Carbon, 17(2), 157-174.
14. Zhou, P., Li, Z. Q., Zhao, H. S., Zhang, K. H., Liu, X. X., & Liu, B. (2016). Sintering of SiC coating layer on graphite spheres prepared by pack cementation. In Key Engineering Materials (Vol. 697, pp. 807-813). Trans Tech Publications Ltd.
15. Choy, K. L. (2003). Chemical vapour deposition of coatings. Progress in materials science, 48(2), 57-170.
16. Jian-Feng, H., Xie-Rong, Z., He-Jun, L., Xin-Bo, X., & Ye-Wei, F. (2004). Influence of the preparation temperature on the phase, microstructure and anti-oxidation property of a SiC coating for C/C composites. Carbon, 42(8-9), 1517-1521.
17. Morimoto, T., Ogura, Y., Kondo, M., & Ueda, T. (1995). Multilayer coating for carbon-carbon composites. Carbon, 33(4), 351-357.
18. Khalife Soltani, S. A., & Azadbeh, M. (2021). Investigation of the high-temperature oxidation behavior of three-dimensional C/C composite and graphite coated by silicon carbide. Advanced Composite Materials, 30(6), 517-526.
19. Paccaud, O., & Derré, A. (2001). Reactive pack-cementation coating of silicon carbide on carbon-carbon composite. Le Journal de Physique IV, 11(PR3), Pr3-1095.
20. Lin, Y. J., & Chen, L. J. (2000). Oxidation of SiC powders in SiC/alumina/zirconia compacts. Ceramics international, 26(6), 593-598.
21. Paccaud, O., & Derre, A. (2000). Silicon carbide coating by reactive pack cementation—part I: silicon carbide/silica interaction. Chemical Vapor Deposition, 6(1), 33-40.
22. Paccaud, O., & Derre, A. (2000). Silicon carbide coating by reactive pack cementation—part II: silicon monoxide/carbon reaction. Chemical Vapor Deposition, 6(1), 41-50.
23. Vetrivendan, E., Madhura, B., Rao, C. J., & Ningshen, S. (2019). Pack cemented silicon carbide interlayer for plasma sprayed yttria over graphite. Materials and Manufacturing Processes, 34(6), 681-688.
24. Morgan, P. (2005). Carbon fibers and their composites. CRC press.
25. Jian-Feng, H., Xie-Rong, Z., He-Jun, L., Xin-Bo, X., & Min, H. (2003). Mullite-Al2O3-SiC oxidation protective coating for carbon/carbon composites. Carbon, 41(14), 2825-2829.
26. Aliasgarian, R., Naderi, M., Mirsalehi, S. E., & Safi, S. (2018). The ablation and oxidation behaviors of SiC coatings on graphite prepared by slurry sintering and pack cementation. Journal of Materials Engineering and Performance, 27(8), 3900-3910.
27. Mirhabibi, A., Shirani, M., & Aghababazadeh, R. (2012). Development of silicon carbide coating on high density graphite by pack cementation process. Carbon.
28. Li, J., & Riedel, R. (2007). Carbothermal reaction of silica–phenol resin hybrid gels to produce silicon nitride/silicon carbide nanocomposite powders. Journal of the American Ceramic Society, 90(12), 3786-3792.
29. Manocha, L. M., Patel, B., & Manocha, S. (2007). Silicon Carbide Coating on Graphite and Isotropic C/C Composite by Chemical Vapour Reaction. Carbon letters, 8(2), 91-94.
30. Abdollahi, A., & Ehsani, N. (2017). C/SiC gradient oxidation protective coating on graphite by modified reactive melt infiltration method: effects of processing parameters on transition interface thickness and high-temperature anti-oxidation behavior. Metallurgical and Materials Transactions A, 48(1), 265-278.

Copyright: *©2022 F Z Mohammad, et al. This is an open-access article distributed under the terms of the Creative Commons Attribution License, which permits unrestricted use, distribution, and reproduction in any medium, provided the original author and source are credited.*